

Using normal forms to study Oterma's transition in the Planar RTBP*

Gladston Duarte^(1,2) and Àngel Jorba⁽¹⁾

16th September 2021

- (1) Departament de Matemàtiques i Informàtica, Universitat de Barcelona (UB) and
Barcelona Graduate School of Mathematics (BGSMath)
Gran Via de les Corts Catalanes 585, 08007 Barcelona, Spain.
- (2) Faculty of Applied Mathematics, AGH University of Science and Technology
Aleja Adama Mickiewicza 30, 30-059, Kraków, Poland.
- E-mails: <gladston@maia.ub.es>, <duarteg@agh.edu.pl>, <angel@maia.ub.es>.

Abstract

Comet 39P/Oterma is known to make fast transitions from an heliocentric orbit outside the orbit of Jupiter to an heliocentric orbit inside that of Jupiter and vice versa. In this note the dynamics of Oterma is quantitatively studied via an explicit computation of high order Birkhoff normal forms at the points L_1 and L_2 of the Planar Restricted Three-Body Problem. Previous works [KLMR01] have shown the existence of heteroclinic connections between the neighbourhood of L_1 and L_2 which provide paths for this transition. Here we combine real data on the motion of Oterma with normal forms to compute the invariant objects that are responsible for this transition.

Keywords : Lagrangian points; Normal form computation; Comet 39P/Oterma.

Contents

1	Introduction	2
2	Normal Forms at L_1 and L_2	5
3	Projecting Oterma on the RTBP	8
4	Oterma in normal form coordinates	9
5	Summary and conclusions	12
	References	13

*This work has been supported by the Spanish grant PGC2018-100699-B-I00 (MCIU/AEI/FEDER, UE) and the Catalan grant 2017 SGR 1374. The project leading to this application has received funding from the European Union's Horizon 2020 research and innovation programme under the Marie Skłodowska-Curie grant agreement #734557. G. D. acknowledges the support from the Spanish Ministry of Economy and Competitiveness through the "María de Maeztu" Programme for Units of Excellence in R&D (MDM-0445-2014) and the support of Polish National Science Centre grant 2018/29/B/ST1/00109.

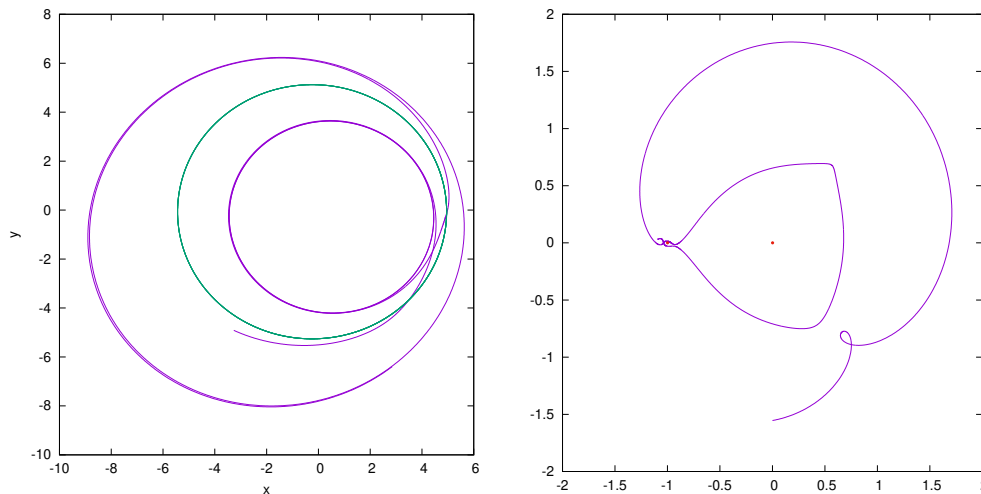


Figure 1: Transition in Oterma’s trajectory shown in sidereal coordinates (left) and in synodical ones (right), both in purple. On the left, Jupiter’s orbit is plotted in green. On the right, Jupiter’s and Sun’s positions are plotted in red.

1 Introduction

It is well known that some comets experience a rapid transition between heliocentric orbits inside and outside of the orbit of Jupiter. A well known example of this transition is given by the comet 39P/Oterma, which has experienced several transitions of this kind ([HB98]). Other comets with a similar behaviour are 82P/Gehrels, 36P/Whipple, 129P/Shoemaker-Levy 3 and 147P/Kushida-Muramatsu ([OIY⁺08]). As an example of this transition, Figure 1 (left) shows the trajectory of 39P/Oterma (in purple) and Jupiter (in green) projected to sidereal (x, y) coordinates (being the xOy reference plane the ecliptic and mean equinox of reference epoch (JD 2452200.5) and the reference frame ICRF/J2000.0 in JPL Horizons Web-Interface). The starting point of this trajectory corresponds to the positions of the bodies on August 30, 1935 when a transition of Oterma is about to happen.

This transition has been modelled using the Planar Circular Restricted Three-Body Problem (from now on, RTBP) in [KLMR01]. In this work, this problem is studied in a qualitative way, i.e., the paper explains a mechanism that permits Oterma to experience the phenomenon of transition between orbits inside and outside the orbit of Jupiter. Such mechanism is known as Rapid Transition Mechanism and it is characterized by a transition without completing a revolution around Jupiter.

The RTBP is a special configuration of the n -Body Problem, with $n = 3$: It is considered that two of the masses (usually called primaries) revolve in circular orbits around their common centre of mass and the third one is assumed to have a negligible mass, so that it is affected by the gravity of the primaries, but it does not affect them. The goal of the RTBP is to describe the motion of the massless particle. In this paper we restrict the motion of this particle to the same plane of movement as the primaries.

Usually, two reference frames are considered for this problem, namely the sidereal and the synodical reference systems. The sidereal system of coordinates is an inertial frame, with origin at the centre of mass, and with axis defined in a suitable way. For instance, when dealing with situations coming from the Solar System, the most common ones are the Ecliptic coordinates (uses

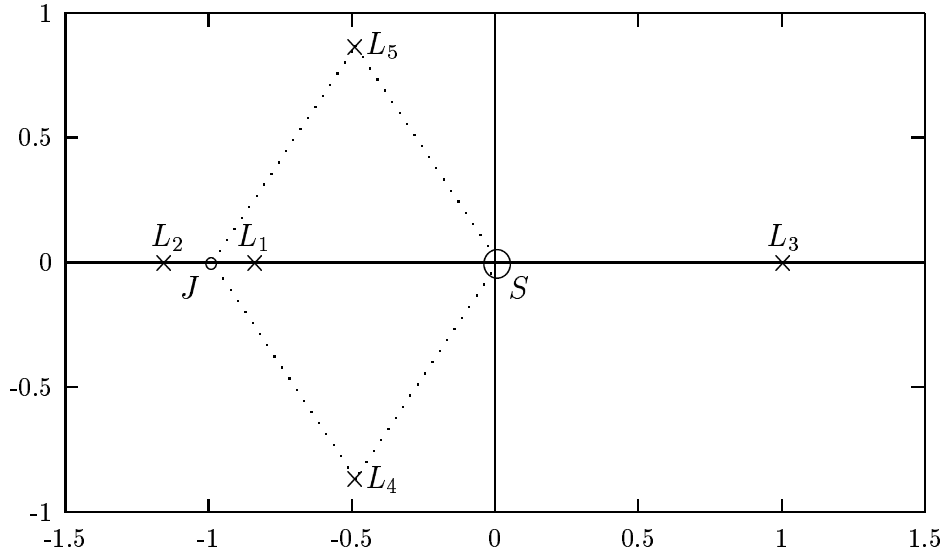


Figure 2: The five equilibrium points of the RTBP.

as the horizontal plane the one defined by Earth's orbit) and the Equatorial coordinates (uses the Earth Equator plane as horizontal plane).

The synodical system of coordinates, in the case of a circular problem, is defined as a system that revolves with the same constant angular velocity as the primaries; the x -axis is defined as the line between the primaries, oriented from the less massive to the more massive one; the z -axis is parallel to the angular momentum vector; and the y -axis is defined accordingly in order to have a positive oriented reference frame. It is also usual to select the unit of distance, time and mass such that the gravitational constant is 1, their period is 2π and the sum of their masses also equals 1. As a consequence, the distance between the primaries is also 1. In these coordinates, the primaries do not move, they stand still in two points: the less massive one in $(-1 + \mu, 0, 0)$ and the more massive one in $(\mu, 0, 0)$ ([Sze67]). In this reference frame, the motion of the massless particle is described by the following Hamiltonian,

$$H(x, y, p_x, p_y) = \frac{1}{2}(p_x^2 + p_y^2) + yp_x - xp_y - \frac{1-\mu}{r_1} - \frac{\mu}{r_2}, \quad (1)$$

where $r_1 = (x-\mu)^2 + y^2$ and $r_2 = (x+1-\mu)^2 + y^2$. This is a 2 degrees-of-freedom autonomous Hamiltonian system, which means that its phase space is four-dimensional foliated by three-dimensional submanifolds each one associated with a value of the Hamiltonian.

It is also well-known that the RTBP has 5 equilibrium points, called L_i , $i = 1, \dots, 5$, three of them located at the x -axis, L_2 to the left of the mass located at $(-1 + \mu, 0, 0)$, L_1 between the primaries and L_3 to the right of the one located at $(\mu, 0, 0)$; and the other two are the third vertex of the two equilateral triangles where the other two vertices are the primaries, one with positive y value, and the other one with negative y , see Figure 2.

A classical constant of motion for the RTBP is the Jacobi constant, that can be defined as $C = -2H$, where H is the Hamiltonian function. Using velocities instead of momenta, it takes the form

$$C = 2\Omega(x, y) - (\dot{x}^2 + \dot{y}^2), \quad \Omega(x, y) = \frac{1}{2}(x^2 + y^2) + \frac{1-\mu}{r_1} + \frac{\mu}{r_2}.$$

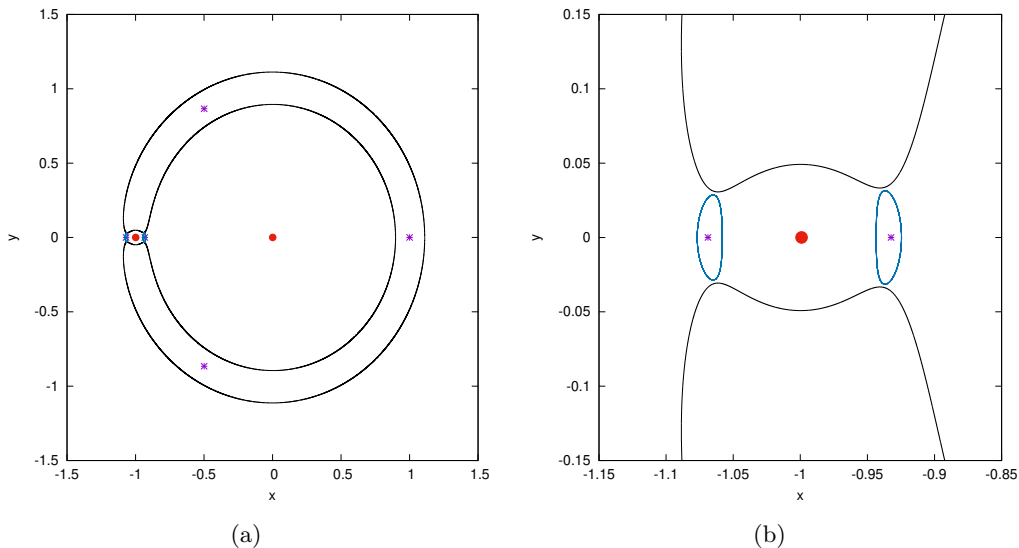


Figure 3: ZVC (in blue), equilibrium points (in purple) and periodic orbits around L_1 and L_2 (in blue) in the RTBP.

For a given value of C , as $\dot{x}^2 + \dot{y}^2 \geq 0$, the motion can only take place in the subset of the configuration space defined by $2\Omega(x, y) - C \geq 0$. The boundaries of this set, $2\Omega(x, y) = C$, are the so called Zero-Velocity Curves or ZVC for short ([Sze67]). For Oterma's case (see [KLMR01]), the ZVC are illustrated in Figure 3. The region enclosed by the black curve corresponds to $2\Omega(x, y) - C < 0$ so the motion cannot take place there. In the complementary set we have drawn two periodic orbits (in blue).

Some key objects to explain Oterma's dynamics are the periodic orbits around the equilibrium points L_1 and L_2 and their stable/unstable manifolds. These points are linearly unstable being of centre \times saddle type, and due to the Lyapunov centre theorem [MO17] there exist a family of periodic orbits born at the centre direction of each point, that can be parametrized by the value of the Hamiltonian. Each of these periodic orbits is hyperbolic and has stable and unstable manifolds. In [KLMR01] it is shown that the intersections between manifolds of the periodic orbits of L_1 with those of periodic orbits of L_2 (and viceversa) explain the transition between regimes.

The goal of this paper is to do a detailed study of the transition for the Oterma case, identifying the concrete periodic orbits and manifolds involved in the transition. To this end we adapt the methods and software of [Jor99] to compute a Birkhoff normal form of degree 60 at the points L_1 and L_2 , and the corresponding changes of variables from synodical coordinates to normal form coordinates and viceversa. It is worth noting that, as $L_{1,2}$ are centre \times saddle points, this normalising process is convergent ([Mos58]). Then, the position of Oterma is translated first from the Solar system reference frame to synodical RTBP coordinates, and then to normal form coordinates so that it becomes evident which objects are relevant for its motion.

This paper is structured as follows: In Section 2 we explain how to adapt the system explained in [Jor99] in order to compute the normal forms at L_1 and L_2 points, in Section 3 we explain the change of variables used to fit Oterma's data in the synodical system of coordinates, i.e., we explain a change of variables from sidereal to synodical in the RTBP, in Section 4 we see how this machinery of normal forms computation can be applied to compute the points in Oterma's orbit from the synodical to normal forms coordinates, and which objects are related to the motion of

Oterma.

2 Normal Forms at L_1 and L_2

The normal form computation is based on the methods and software in [Jor99] but with some changes to adapt them to the present situation. To facilitate the reading, in this section we summarise the methods in [Jor99] and the modifications we have done to adapt them to this case.

As usual, the first step is to translate the origin to the point L_1 or L_2 . This is done by means of a translation,

$$\begin{cases} X &= -\gamma_j x + \mu + \alpha_j, \\ Y &= -\gamma_j y, \\ Z &= \gamma_j z, \end{cases} \quad \begin{cases} P_X &= -\gamma_j p_x, \\ P_Y &= -\gamma_j p_y + \mu + \alpha_j, \\ P_Z &= \gamma_j p_z, \end{cases} \quad (2)$$

where the uppercase letters represent the synodical coordinates and the lowercase ones the coordinates centered at the collinear point. Here γ_j denotes the only positive solution of the Euler quintic equation,

$$\gamma_j^5 \mp (3 - \mu)\gamma_j^4 + (3 - 2\mu)\gamma_j^3 - \mu\gamma_j^2 \pm 2\mu\gamma_j - \mu = 0,$$

for $j = 1, 2$ where the upper sign is for $j = 1$ and the lower one, for $j = 2$ (see, for instance, [Sze67]), and $\alpha_j = -1 + (-1)^{j+1}\gamma_j$. We note that, at the same time, we have done a scaling on the distances. The goal of this scaling is that the power expansions have a radius of convergence 1 which avoids very large or very small coefficients in these expansions and this helps reducing the error propagation [Ric80]. As this change of variables is not canonical, it has to be applied to the differential equations and then to recover a Hamiltonian function.

Then, a linear canonical change of variables is used to rearrange the second order terms. As $L_{1,2}$ are of centre \times saddle type, these terms take the form

$$H_2 = \lambda x_1 y_1 + \frac{\omega}{2}(x_2^2 + y_2^2),$$

where (x_1, x_2) are the new positions and (y_1, y_2) are the momenta. To simplify the normalizing transformations, it is usual to use complex variables for the elliptic directions,

$$x_2 = \frac{q_2 + i p_2}{\sqrt{2}}, \quad x_2 = \frac{i q_2 + p_2}{\sqrt{2}}, \quad (3)$$

so that H_2 becomes ‘‘diagonal’’,

$$H_2 = \lambda q_1 p_1 + i \omega q_2 p_2,$$

where to simplify the notation we have renamed (x_1, y_1) as (q_1, p_1) . Then, the Hamiltonian is expanded in power series in these variables by means of suitable recurrences [JM99], to obtain

$$H = H_2 + H_3 + \cdots + H_m + O_{m+1}, \quad (4)$$

where H_j is an homogeneous polynomial of degree j in the variables (q_1, q_2, p_1, p_2) . Next step is to perform a Birkhoff normalization. It is based on a sequence of canonical transformations that rearrange the power expansion (4) degree by degree. It is well-known that the time t flow of a Hamiltonian system G is a canonical transformation Φ_t^G and that

$$H \circ \Phi_t^G = H + t \{H, G\} + \frac{t^2}{2!} \{\{H, G\}, G\} + \frac{t^3}{3!} \{\{\{H, G\}, G\}, G\} + \cdots, \quad (5)$$

where $\{\cdot, \cdot\}$ denotes the usual Poisson bracket: if $P = P(q, p)$ and $Q = Q(q, p)$ are two smooth functions, then

$$\{P, Q\} = \sum_{j=1}^2 \frac{\partial P}{\partial q_j} \frac{\partial Q}{\partial p_j} - \frac{\partial P}{\partial p_j} \frac{\partial Q}{\partial q_j}.$$

Of course, expression (5) is only valid on the domain of convergence of this expansion (see, for instance, [MO17]). As H is a truncated power expansion, and we will choose G as a polynomial, the expression (5) can be easily implemented on a computer and, therefore, it is very suitable for effective computations. Let us see how it is applied.

We start by degree 3. This means that we use an homogeneous polynomial of degree 3, G_3 , to transform (4). At this point we note that if P and Q are homogeneous polynomials of degree r and s , then $\{P, Q\}$ is an homogeneous polynomial of degree $r + s - 2$. If we denote \hat{H} as $H \circ \Phi_t^{G_3}$ and \hat{H}_j denotes the terms of degree j of the power expansion of \hat{H} , then

$$\hat{H}_2 = H_2, \quad \hat{H}_3 = H_3 + \{H_2, G_3\}, \quad \hat{H}_4 = H_4 + \{H_3, G_3\} + \frac{1}{2!} \{\{H_2, G_3\}, G_3\},$$

and so on. To find G_3 let us write

$$H_3(q, p) = \sum_{|k|=3} h_k q^{k_q} p^{k_p}, \quad G_3(q, p) = \sum_{|k|=3} g_k q^{k_q} p^{k_p},$$

where $h_k, g_k \in \mathbb{C}$, $k = (k_1, \dots, k_4)$, $k_j \in \mathbb{N}_0$, $k_q = (k_1, k_2)$, $q^{k_q} = q_1^{k_1} q_2^{k_2}$ and similarly for k_p and p^{k_p} . It is not difficult to find a G_3 such that $\hat{H}_3 \equiv 0$,

$$G_3(q, p) = \sum_{|k|=3} \frac{-h_k}{\langle k_p - k_q, (\lambda, i\omega) \rangle}.$$

Note that $|k| = 3$ implies that $k_p \neq k_q$ and then the denominator above has to be different from zero. To simplify notation, let us denote \hat{H} as H , the transformed Hamiltonian has the form

$$H = H_2 + H_4 + \dots + H_m + O_{m+1}, \tag{6}$$

Transforming this last Hamiltonian by the flow of G_4 we obtain

$$\hat{H}_2 = H_2, \quad \hat{H}_4 = H_4 + \{H_2, G_4\},$$

and so on. If now we try to remove \hat{H}_4 using a suitable G_4 we need to choose G_4 as

$$G_4(q, p) = \sum_{|k|=4} \frac{-h_k}{\langle k_p - k_q, (\lambda, i\omega) \rangle},$$

but now some of the divisors can be zero: as $|k| = 4$, the monomials with $k_q = k_p$ produce a vanishing denominator and hence they cannot be removed from the Hamiltonian. For the generic case, it is not difficult to see that if the degree is odd all monomials can be removed, and when the degree is even some monomials remain (those with $k_q = k_p$). The result of this process, up to a given degree m (even), is a Hamiltonian of the form

$$H = H_2 + H_4 + H_6 + \dots + H_m + O_{m+1},$$

and the only remaining monomials are those with $k_q = k_p$. Skipping the remainder O_{m+1} we obtain an integrable Hamiltonian. To see it, let us go back first to real coordinates using the inverse of the complexifying change (3),

$$q_2 = \frac{x_2 - i y_2}{\sqrt{2}}, \quad p_2 = \frac{-i x_2 + y_2}{\sqrt{2}}. \quad (7)$$

As (q_1, p_1) are already real we simply rename them as (x_1, y_1) to simplify the notation. To put the Hamiltonian in action-angle coordinates we use, for the elliptic direction,

$$x_2 = \sqrt{2I_2} \cos \varphi_2, \quad y_2 = -\sqrt{2I_2} \sin \varphi_2, \quad (8)$$

and, for the hyperbolic directions,

$$x_1 = \sqrt{I_1} \exp(\varphi_1), \quad y_1 = \sqrt{I_1} \exp(-\varphi_1). \quad (9)$$

Here φ_1 is a hyperbolic angle, whose relation with a hyperbola is similar to the relation of a standard angle with the circle. With this last (symplectic) change, the Hamiltonian is a power expansion of the actions $I_{1,2}$ with real coefficients that do not depend on $\varphi_{1,2}$ (this is because only monomials with $k_q = k_p$ are present) so it is integrable. We recall that, as L_1 and L_2 are of center \times saddle type, this normal form is convergent [Mos58]. In particular, its construction does not involve small divisors. As usual, we also compute the normalizing change of variables (direct and inverse), so we can send points from the normal form coordinates to synodical coordinates of the RTBP and viceversa, provided that the data is inside the domain of convergence of the expansions. The main difference with [Jor99] is that there the normal form is performed at an elliptic point while here is a saddle \times centre point. Although the normalizing process is exactly the same, the final transformation to action-angle variables is different due to the hyperbolic directions.

Assume that the final Hamiltonian is $H = H(I_1, I_2)$ and let us comment on the role of the two action variables. Setting $I_2 = 0$ we have a family of hyperbolic motions that are described by

$$I_1 = I_1^{(0)}, \quad \varphi_1 = \lambda(I_1^{(0)}, 0)t + \varphi_1^{(0)}, \quad \lambda(I_1^{(0)}, 0) = \frac{\partial H}{\partial I_1}(I_1^{(0)}, 0).$$

We note that φ_1 is an hyperbolic angle. This means that to go to cartesian coordinates we have to use (9) and then φ_1 parametrizes the corresponding hyperbola in the (x_1, y_1) plane. The case of the stable/unstable manifolds of the equilibrium point corresponds to the limit case $I_1 = 0$, and they are given by $(x_1(t), y_1(t)) = (\exp[\lambda(0, 0)t + \varphi_1^{(0)}], 0)$ the unstable manifold, and by $(x_1(t), y_1(t)) = (0, \exp[-\lambda(0, 0)t - \varphi_1^{(0)}])$ the stable one. On the other hand, setting $I_1 = 0$ (and letting $I_2 > 0$) restricts the dynamics to the family of planar Lyapunov orbits, that are described by

$$I_2 = I_2^{(0)}, \quad \varphi_2 = \omega(0, I_2^{(0)})t + \varphi_2^{(0)}, \quad \omega(0, I_2^{(0)}) = \frac{\partial H}{\partial I_2}(0, I_2^{(0)}),$$

and we can use (8) to go to cartesian coordinates. The action I_2 parametrizes the family of Lyapunov orbits, starting at $I_2 = 0$ (the equilibrium point, being $\omega(0, 0)$ the linear frequency at the point). We note that the invariant manifolds of this periodic orbit also satisfy $I_1 = 0$ (they belong to the same energy level as the periodic orbit). Then, the periodic orbit is given by

$$(x_2(t), y_2(t)) = (\sqrt{2I_2^{(0)}} \cos(\omega(0, I_2^{(0)})t + \varphi_2^{(0)}), -\sqrt{2I_2^{(0)}} \sin(\omega(0, I_2^{(0)})t + \varphi_2^{(0)})),$$

and its stable/unstable manifolds are

$$(x_1(t), y_1(t)) = (\exp[\lambda(0, I_2^{(0)})t + \varphi_1^{(0)}], 0) \quad \text{and} \quad (x_1(t), y_1(t)) = (0, \exp[-\lambda(0, I_2^{(0)})t - \varphi_1^{(0)}]),$$

where $\varphi_2^{(0)}$ is an initial phase on the periodic orbit and $\varphi_1^{(0)}$ is an ‘‘initial phase’’ on the manifold.

Therefore, from the normal form we have an accurate computation of the Lyapunov family of periodic orbits as well as their stable/unstable manifolds, in a suitable neighbourhood of the equilibrium point where this normal form converges. These periodic orbits and manifolds can be translated to the initial synodical coordinates by means of the changes of variables.

To extend the manifolds beyond the domain of validity of the normal form, we can take a mesh of initial conditions on the manifold, send this mesh to synodical coordinates and integrate these initial conditions to obtain a set of orbits on the manifolds that allow to visualise the global behaviour of the manifold. For instance, for the unstable manifold of the Lyapunov orbit $I_1 = 0$, $I_2 = I_2^{(0)}$ we can use the mesh

$$(x_1, y_1, x_2, y_2) = (\pm\sigma_0, 0, \sqrt{2I_2^{(0)}} \cos \frac{2\pi k}{N}, \sqrt{2I_2^{(0)}} \sin \frac{2\pi k}{N}), \quad k = 0, \dots, N-1, \quad (10)$$

for a value $\sigma_0 > 0$ such that the points are inside the domain of validity of the normal form (each of the signs \pm is used for each side of the manifold). Similarly, for the stable manifold we use

$$(x_1, y_1, x_2, y_2) = (0, \pm\sigma_0, \sqrt{2I_2^{(0)}} \cos \frac{2\pi k}{N}, \sqrt{2I_2^{(0)}} \sin \frac{2\pi k}{N}), \quad k = 0, \dots, N-1. \quad (11)$$

The normal form has been computed up to order 60 in cartesian coordinates (which means up to order 30 in actions). Several numerical tests have shown that the standard double precision arithmetic of the computer is not precise enough to produce accurate coefficients for the last terms of the expansion. Therefore, we have used quadruple precision for the coefficients, which has been sufficient to obtain accurate values in double precision. The resulting normal form and changes of variables have been stored and then used in double precision.

3 Projecting Oterma on the RTBP

At some given time, we have to take the position and velocity of Oterma in the Solar system and translate them to the planar RTBP. This step is not trivial since in the RTBP, Sun and Jupiter revolve in circular orbits around their centre of mass, while in the real system they have a different motion. Note that, if at a given time, we take the real positions and velocities of Sun, Jupiter and Oterma and assume that, from this moment on, the rest of the Solar system is ignored, then the motion of Sun and Jupiter will not be circular but elliptic. In this section we discuss how we transport the position of Oterma to the planar RTBP.

Let us first give the process we have followed for this transformation of coordinates ([GLMS01]), and then we will discuss the particularities for this case. The positions of Sun, Jupiter and Oterma’s data are gathered from the online system JPL Horizons [JPL] on August 30, 1935 as the initial time. At this date, Oterma is about to experience a transition (see Figure 1) from outside to the inside of the orbit of Jupiter. If we choose as origin of time ($t = 0$) the date January 1, 2000, the chosen date becomes $t = -23500$. At this date, the angle between the Sun-Oterma line and the (instantaneous) plane of motion of Jupiter is of 2.486 degrees, which makes reasonable to use a planar model as in [KLMR01]. The main steps of the process are:

x	$-1.0952439413131636 \times 10^0$
y	$2.9918455882452549 \times 10^{-2}$
p_x	$8.0698975794308611 \times 10^{-1}$
p_y	$-1.0358302646539692 \times 10^0$

Table 1: Oterma’s positions and momenta used as initial conditions in the RTBP.

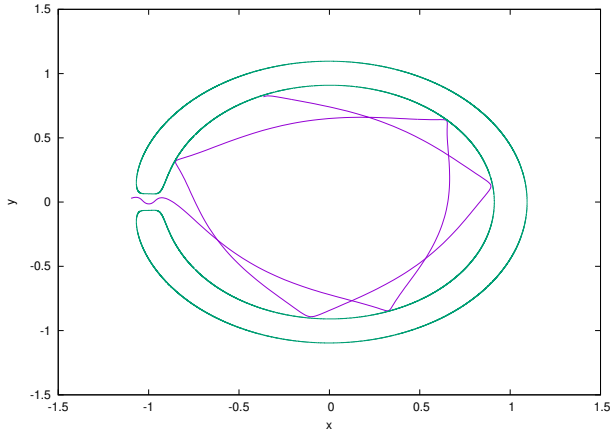


Figure 4: Oterma’s orbit using the data in Table 1 as initial conditions.

- Project orthogonally both Oterma’s position and velocity onto the plane where Sun and Jupiter move. This is done by applying the formulas: $\vec{r} \leftarrow \vec{r} - \langle \vec{r}, \vec{n} \rangle \vec{n}$ and $\vec{v} \leftarrow \vec{v} - \langle \vec{v}, \vec{n} \rangle \vec{n}$, where \vec{n} is the unitary normal vector to the Sun-Jupiter’s movement plane.
- Rotate (in space) the plane defined by the positions and velocities of Sun and Jupiter so that it is now the xOy plane.
- Inside that plane, rotate x and y axes such that both Jupiter and Sun are on the x axis.
- Change the units of position and velocity so that Jupiter is fixed at $(-1 + \mu, 0, 0)$, Sun is fixed at $(\mu, 0, 0)$ and Jupiter’s period of revolution is 2π . To this end, (i) divide the Sun-Jupiter distance (r_{SJ}) and Sun-Oterma distance (r_{SO}) by r_{SJ} , so that r_{SJ} is 1; (ii) divide the velocity of Oterma by $n \times r_{SJ}$, where n is the mean motion of Jupiter, so that the time needed for a complete revolution of Jupiter is 2π ; and (iii) apply the formulas $\dot{x} = p_x + y$, $\dot{y} = p_y - x$ to compute Oterma’s momenta.

After these transformations, the initial data for Oterma in RTBP coordinates is presented in Table 1. The corresponding RTBP orbit is displayed in Figure 4. Comparing Figures 1 and 4 it is clear that the planar RTBP is a good simplified model to study the transition from the outside to the inside region, which is the focus of this paper.

4 Oterma in normal form coordinates

In this section we analyse which invariant objects organise the transition of Oterma near L_1 and L_2 . To this end, when the orbit is close to $L_{1,2}$, we transform the coordinates of some points on the orbit to the normal form coordinates. Note that the normal form has a limited radius of convergence, so we can only use points on the orbit that are sufficiently close to L_1 or L_2 . Therefore, we integrate

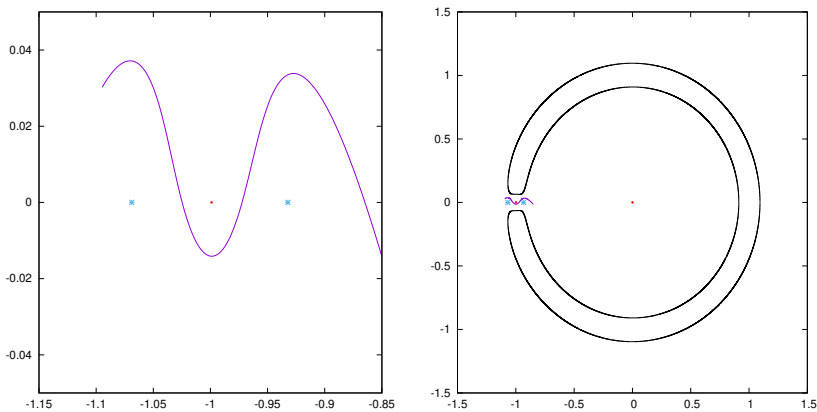


Figure 5: Oterma's orbit in RTBP synodical (x, y) positions, near L_1 and L_2 .

the initial conditions in Table 1 while the orbit is close to $L_{1,2}$ as shown in Figure 5, where a total number of 406 points along the orbit are used. They are integrated using a Taylor integrator [JZ05] of order 20 using a fixed step of 5×10^{-3} such that the relative and absolute tolerances of 10^{-16} are satisfied.

Then, we use a normal form up to order 60 (order 30 in action variables $I = (I_1, I_2)$) at each of the points L_1 and at L_2 , and we transform the coordinates of the points shown in Figure 6 that are close to $L_{1,2}$. To estimate the error due to the truncation to order 60 of the expansions (recall that the orbit could be close to the boundary of the domain of convergence of these power series) we check the contribution of the monomials of higher degree. Tables 2 and 3 show the values of both actions $I_1 = q_1 p_1$, $I_2 = (q_2^2 + p_2^2)/2$ together with the sum of the terms of degree 30 of the Hamiltonian in the action variables (let us call this quantity h_{30}) for the change in each variable for some points in Oterma's integrated orbit, where the conservation of both action variables is better seen.

As it can be seen from Tables 2 and 3 the conservation of the actions variables I_1 and I_2 is close to 10^{-14} and the sum of the monomials of highest degree evaluated at these points is even smaller. This shows that this conservation is of the order of the error of the numerical integration of the orbit. In addition to these points shown in Tables 2 and 3 we have also estimated the truncation error of the change of variables from normal form to cartesian coordinates at several orders, by computing the size of the contribution at the maximum degree for several orders, say 24, 32, 40, 48 and 56. We have used the initial data between highlighted black lines in the middle of Tables 2 and 3. The results are shown in Table 4. Note that, for the conservation of I_1 and I_2 , the orders decrease two orders of magnitude as we increase 8 orders of the normal forms, starting from 10^{-8} using order 24 until 10^{-14} using orders 48, 56 and 60.

When the orbit is inside the domain of convergence of the normal form we can easily compute the periodic orbits involved in this transition. For instance, computing

$$\left. \frac{\partial H}{\partial I_2} \right|_{(0, I_2^*)},$$

where the point $(0, I_2^*)$ is, for the computations around L_1 , $I_2^* = 4.2878140057480268 \times 10^{-1}$ (corresponding to the point with $t = -23498.63$, see Table 2) and for the computations around L_2 , $I_2^* = 4.1263461076678953 \times 10^{-1}$ (corresponding to the point with $t = -23499.62$, see Table 3), we obtain the frequencies of these periodic orbits, 2.0645952307976740 and 1.9048266439827066. The

t	$I_1 = q_1 p_1$	$I_2 = (q_2^2 + p_2^2)/2$	h_{30}
-23498.68	$2.3735585604354004 \times 10^{-1}$	$4.2878140057480135 \times 10^{-1}$	1.127×10^{-20}
-23498.675	$2.3735585604354054 \times 10^{-1}$	$4.2878140057480163 \times 10^{-1}$	1.127×10^{-20}
-23498.67	$2.3735585604354045 \times 10^{-1}$	$4.2878140057480196 \times 10^{-1}$	1.127×10^{-20}
-23498.665	$2.3735585604354040 \times 10^{-1}$	$4.2878140057480207 \times 10^{-1}$	1.127×10^{-20}
-23498.66	$2.3735585604354045 \times 10^{-1}$	$4.2878140057480213 \times 10^{-1}$	1.127×10^{-20}
-23498.655	$2.3735585604354040 \times 10^{-1}$	$4.2878140057480219 \times 10^{-1}$	1.127×10^{-20}
-23498.65	$2.3735585604354040 \times 10^{-1}$	$4.2878140057480213 \times 10^{-1}$	1.127×10^{-20}
-23498.645	$2.3735585604354062 \times 10^{-1}$	$4.2878140057480230 \times 10^{-1}$	1.127×10^{-20}
-23498.64	$2.3735585604354009 \times 10^{-1}$	$4.2878140057480185 \times 10^{-1}$	1.127×10^{-20}
-23498.635	$2.3735585604354056 \times 10^{-1}$	$4.2878140057480202 \times 10^{-1}$	1.127×10^{-20}
-23498.63	$2.3735585604354006 \times 10^{-1}$	$4.2878140057480268 \times 10^{-1}$	1.127×10^{-20}
-23498.625	$2.3735585604353993 \times 10^{-1}$	$4.2878140057480224 \times 10^{-1}$	1.127×10^{-20}
-23498.62	$2.3735585604354126 \times 10^{-1}$	$4.2878140057480219 \times 10^{-1}$	1.127×10^{-20}
-23498.615	$2.3735585604354120 \times 10^{-1}$	$4.2878140057480119 \times 10^{-1}$	1.127×10^{-20}
-23498.61	$2.3735585604354051 \times 10^{-1}$	$4.2878140057480241 \times 10^{-1}$	1.127×10^{-20}
-23498.605	$2.3735585604354129 \times 10^{-1}$	$4.2878140057480252 \times 10^{-1}$	1.127×10^{-20}
-23498.6	$2.3735585604353923 \times 10^{-1}$	$4.2878140057480257 \times 10^{-1}$	1.127×10^{-20}
-23498.595	$2.3735585604354037 \times 10^{-1}$	$4.2878140057480124 \times 10^{-1}$	1.127×10^{-20}
-23498.59	$2.3735585604354004 \times 10^{-1}$	$4.2878140057480252 \times 10^{-1}$	1.127×10^{-20}
-23498.585	$2.3735585604354048 \times 10^{-1}$	$4.2878140057480130 \times 10^{-1}$	1.127×10^{-20}
-23498.58	$2.3735585604354170 \times 10^{-1}$	$4.2878140057480124 \times 10^{-1}$	1.127×10^{-20}

Table 2: I_1 , I_2 and h_{30} computed at L_1

t	$I_1 = q_1 p_1$	$I_2 = (q_2^2 + p_2^2)/2$	h_{30}
-23499.67	$1.9332991772006497 \times 10^{-1}$	$4.1263461076678953 \times 10^{-1}$	3.045×10^{-22}
-23499.665	$1.9332991772006392 \times 10^{-1}$	$4.1263461076678948 \times 10^{-1}$	3.045×10^{-22}
-23499.66	$1.9332991772006430 \times 10^{-1}$	$4.1263461076678759 \times 10^{-1}$	3.045×10^{-22}
-23499.655	$1.9332991772006414 \times 10^{-1}$	$4.1263461076678970 \times 10^{-1}$	3.045×10^{-22}
-23499.65	$1.9332991772006439 \times 10^{-1}$	$4.1263461076678870 \times 10^{-1}$	3.045×10^{-22}
-23499.645	$1.9332991772006375 \times 10^{-1}$	$4.1263461076678903 \times 10^{-1}$	3.045×10^{-22}
-23499.64	$1.9332991772006444 \times 10^{-1}$	$4.1263461076678820 \times 10^{-1}$	3.045×10^{-22}
-23499.635	$1.9332991772006430 \times 10^{-1}$	$4.1263461076678898 \times 10^{-1}$	3.045×10^{-22}
-23499.63	$1.9332991772006386 \times 10^{-1}$	$4.1263461076678859 \times 10^{-1}$	3.045×10^{-22}
-23499.625	$1.9332991772006433 \times 10^{-1}$	$4.1263461076678837 \times 10^{-1}$	3.045×10^{-22}
-23499.62	$1.9332991772006486 \times 10^{-1}$	$4.1263461076678953 \times 10^{-1}$	3.045×10^{-22}
-23499.615	$1.9332991772006428 \times 10^{-1}$	$4.1263461076678931 \times 10^{-1}$	3.045×10^{-22}
-23499.61	$1.9332991772006441 \times 10^{-1}$	$4.1263461076678837 \times 10^{-1}$	3.045×10^{-22}
-23499.605	$1.9332991772006436 \times 10^{-1}$	$4.1263461076678865 \times 10^{-1}$	3.045×10^{-22}
-23499.60	$1.9332991772006472 \times 10^{-1}$	$4.1263461076678876 \times 10^{-1}$	3.045×10^{-22}
-23499.595	$1.9332991772006516 \times 10^{-1}$	$4.1263461076678876 \times 10^{-1}$	3.045×10^{-22}
-23499.59	$1.9332991772006516 \times 10^{-1}$	$4.1263461076678898 \times 10^{-1}$	3.045×10^{-22}
-23499.585	$1.9332991772006580 \times 10^{-1}$	$4.1263461076678898 \times 10^{-1}$	3.045×10^{-22}
-23499.58	$1.9332991772006619 \times 10^{-1}$	$4.1263461076678942 \times 10^{-1}$	3.045×10^{-22}
-23499.575	$1.9332991772006589 \times 10^{-1}$	$4.1263461076678914 \times 10^{-1}$	3.045×10^{-22}
-23499.57	$1.9332991772006602 \times 10^{-1}$	$4.1263461076678926 \times 10^{-1}$	3.045×10^{-22}

Table 3: I_1 , I_2 and h_{30} computed at L_2

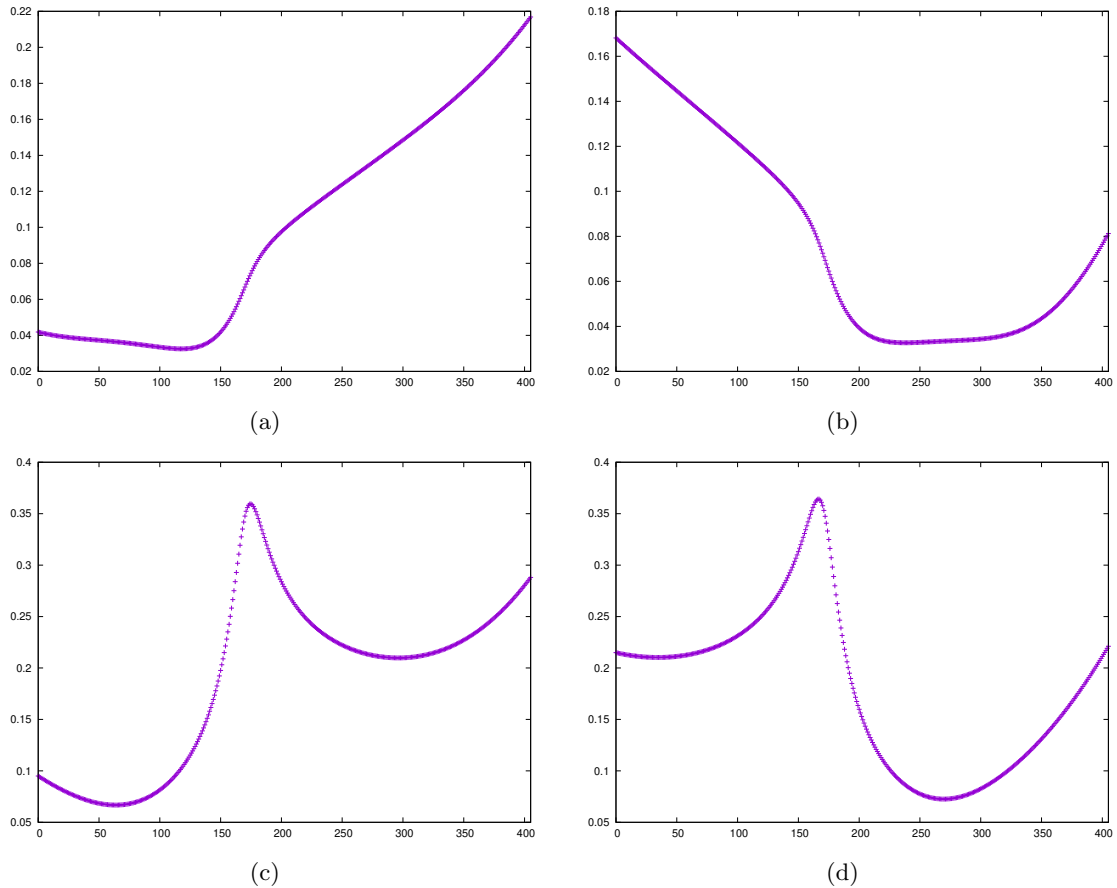


Figure 6: Vertical axis: distance between Oterma and L_1 (right) and L_2 (left) in configuration space (top) and phase space (bottom). Horizontal axis: an index numbering the mesh on points on the orbit.

orbits and their stable/unstable manifolds can be computed accurately, inside the domain of the normal form, using the expressions (10) and (11). If desired, they can be globalised by means of numerical integrations.

5 Summary and conclusions

In this work we have analysed quantitatively, using a normal form approach, the objects involved in Oterma's transition. The computation of the normal forms at L_1 and L_2 were done adapting a public domain code ([Jor99]) for this case. This includes adding the code to handle the hyperbolic directions and to operate with quadruple precision. All the theory involved in this computation is presented in this reference, the only exception being the treatment, in the normal form, of the hyperbolic direction of $L_{1,2}$ which has been included here.

We have also discussed the change of coordinates needed to send data from JPL ephemeris to the RTBP planar model, to highlight the simplifications done when choosing this model. Since we are not interested here in the motion of Oterma far from the transition, we have chosen as initial time a moment when Oterma is about to experience a transition from outside to the inside of the orbit of Jupiter.

	L_1	L_2
Order 24	$7.9760239699283809 \times 10^{-10}$	$2.7765943768364664 \times 10^{-10}$
Order 32	$2.2427370346101517 \times 10^{-12}$	$3.9594494889226486 \times 10^{-13}$
Order 40	$8.1359645807725896 \times 10^{-15}$	$1.0198945467998282 \times 10^{-15}$
Order 48	$2.3883565010998806 \times 10^{-17}$	$1.4307930312682510 \times 10^{-18}$
Order 56	$1.1230484307642622 \times 10^{-19}$	$8.3245178575158536 \times 10^{-21}$
Order 60	$1.1272938164516016 \times 10^{-20}$	$3.0458619961877403 \times 10^{-22}$

Table 4: Comparison between evaluations of the maximum degree monomials of different degrees. For the ones around L_1 the chosen point is the one with $t = -23498.63$, and for the ones around L_2 it is the one with $t = -23499.62$.

As the normal form is convergent in this case, we have used a very high order normal form to obtain an accurate description of a neighbourhood of $L_{1,2}$ to obtain explicitly the periodic orbits and the invariant manifolds involved. This is a complicated task using other methods since it is difficult to identify which are the periodic orbits whose invariant manifolds guide the transition. This identification becomes trivial with the normal form.

As perspectives we cite the works in progress [DJ21a, DJ21b] on which we use as a model the planar Elliptic RTBP (PERTBP) instead of the RTBP used here. The dynamical objects around L_1 and L_2 (invariant tori and their stable/unstable manifolds) in that scenario are much more difficult to compute. In particular, the normal form is no longer convergent. Therefore, the invariant objects around L_1 and L_2 have to be computed using numerical procedures for invariant tori and their invariant manifolds.

References

- [DJ21a] G. Duarte and À. Jorba. Invariant manifolds of tori near L_1 and L_2 in the Planar Elliptic RTBP. In preparation, 2021.
- [DJ21b] G. Duarte and À. Jorba. Modelling Oterma’s transition using the Planar Elliptic RTBP. In preparation, 2021.
- [GLMS01] G. Gómez, J. Llibre, R. Martínez, and C. Simó. *Dynamics and mission design near libration points. Vol. I, Fundamentals: the case of collinear libration points*, volume 2 of *World Scientific Monograph Series in Mathematics*. World Scientific Publishing Co. Inc., 2001.
- [HB98] N.W. Harris and M.E. Bailey. Dynamical evolution of cometary asteroids. *Mon. Not. R. Astron. Soc.*, 297(4):1227–1236, 07 1998.
- [JM99] À. Jorba and J. Masdemont. Dynamics in the centre manifold of the collinear points of the Restricted Three Body Problem. *Phys. D*, 132:189–213, 1999.
- [Jor99] À. Jorba. A methodology for the numerical computation of normal forms, centre manifolds and first integrals of Hamiltonian systems. *Exp. Math.*, 8(2):155–195, 1999.
- [JPL] <http://ssd.jpl.nasa.gov/horizons.html>.
- [JZ05] À. Jorba and M. Zou. A software package for the numerical integration of ODEs by means of high-order Taylor methods. *Exp. Math.*, 14(1):99–117, 2005.

- [KLMR01] W.S. Koon, M.W. Lo, J.E. Marsden, and S.D. Ross. Resonance and capture of Jupiter comets. *Celest. Mech. Dyn. Astron.*, 81(1-2):27–38, 2001.
- [MO17] K.R. Meyer and D. Offin. *Introduction to Hamiltonian dynamical systems and the N-body problem*, volume 90 of *Applied Mathematical Sciences*. Springer, New York, third edition, 2017.
- [Mos58] J. Moser. On the generalization of a theorem of A. Liapounoff. *Comm. Pure Appl. Math.*, 11(2):257–271, 1958.
- [OIY+08] K. Ohtsuka, T. Ito, M. Yoshikawa, D.J. Asher, and H. Arakida. Quasi-Hilda comet 147P/Kushida-Muramatsu - Another long temporary satellite capture by Jupiter. *Astron. Astrophys.*, 489(3):1355–1362, 2008.
- [Ric80] D.L. Richardson. A note on a Lagrangian formulation for motion about the collinear points. *Celestial Mech.*, 22(3):231–236, 1980.
- [Sze67] V. Szebehely. *Theory of Orbits*. Academic Press, 1967.